 doi:10.20944/preprints202011.0404.v1

Communication

An improved method for physical separation of cerebral vasculature and parenchyma enables detection of blood-brain-barrier dysfunction

Frank Matthes [1,2] +, Hana Matuskova [1,2,3,4] +, Kajsa Arkelius [5], Saema Ansar [5], Iben Lundgaard [1,2] and Anja Meissner [1,2,4]*

[1] Department of Experimental Medical Sciences, Lund University, Lund, Sweden
[2] Wallenberg Centre for Molecular Medicine, Lund University, Lund, Sweden
[3] Department of Neurology, University Hospital Bonn, Bonn, Germany
[4] German Center of Neurodegenerative Disease, Bonn, Germany
[5] Department of Clinical Sciences, Lund University, Lund, Sweden

+ Equal contribution
* Correspondence: anja.meissner@med.lu.se; Tel.: +46-46 22 20 641

Abstract: The neurovascular niche is crucial for constant blood supply and blood-brain barrier (BBB) function and is altered in a number of different neurological conditions, making this an intensely active field of research. Brain vasculature is unique for its tight association of endothelial cells with astrocytic endfeet processes. Separation of the vascular compartment by centrifugation-based methods confirmed enrichment of astrocytic endfeet processes, making it possible to study the entire vascular niche with such methods. Several centrifugation-based separation protocols are found in the literature; however, with some constraints which limit their applicability and the scope of the studies. Here, we describe and validate a protocol for physically separating the neurovascular niche from the parenchyma, which is optimized for smaller tissue quantities. Using endothelial, neuronal and astrocyte markers, we show that quantitative Western blot-based target detection can be performed of both the vascular and parenchymal fractions using as little as a single mouse brain hemisphere. Validation of our protocol in rodent stroke models by detecting changes in serum albumin signals and astrocyte activation, i.e. increased glial fibrillary acidic protein expression, between the ipsilateral and the lesion-free contralateral hemisphere demonstrates this protocol as a new way of detecting BBB breakdown and astrogliosis, respectively.

Keywords: Cerebral vasculature, vascular fractionation protocol, neurovascular niche, blood-brain barrier, stroke

1. Introduction

The cerebral vasculature has unique properties since transfer of molecules to the brain parenchyma is tightly regulated by the blood-brain barrier (BBB) [1, 2]. Vascular functions can be impaired in diverse neuropathological conditions [3] thus, not only disturbing proper distribution of metabolites within the brain but also limiting its capability to protect neurotoxic substances from entering the brain [4, 5]. Studies have shown involvement of BBB dysfunctions and cerebral blood flow deficits in the pathogenesis of neurodegenerative diseases such as Alzheimer's disease, Parkinson's disease, and amyotrophic lateral sclerosis [3], [6, 7]. During stroke, disruption of the BBB can lead to secondary damage such as brain edema or hemorrhagic transformation, and to the

Preprints (www.preprints.org) | NOT PEER-REVIEWED | Posted: 16 November 2020 doi:10.20944/preprints202011.0404.v1

infiltration of immune cells [8]. Investigations of brain vasculature in such disease conditions require *in vivo* studies because of the complexity of disease pathologies and the variety of cell types involved. Therefore, research relies in part on animal models, and quantitative methods are needed in order to elaborate the precise mechanisms behind pathology, which in turn eventually leads to the development of new therapeutic strategies.

To study cerebral vasculature, several protocols for purifying mouse brain vessels or generating brain vessel-enriched fractions have been published [9-11]. Purified vessels have been investigated using immunofluorescence stainings and Western blotting, but studies usually focus on the purified vessels alone, without comparison to the remaining brain parenchyma. In a recent study, we used a protocol that was slightly modified from a previously published protocol [9] to study vascular polarization of astrocyte endfeet in platelet-derived growth factor B retention-motif knockout (PDGF-B$^{ret/ret}$) mice during development [12]. Several limitations, including presence of high concentrations of bovine serum albumin and high tissue quantity requirements that necessitated pooling of several mouse brains for Western blot-based quantification led us to further modify the previously published mouse brain vessel isolation method. Our modified method permits Western blot analyses of brain vessel and brain parenchyma fractions from the same tissue sample utilizing only one mouse brain hemisphere, thus enabling investigations requiring the direct comparison of the two brain hemispheres from the same animal, such as in stroke research. Here, we demonstrate the applicability of a modified brain vessel isolation method in a murine and rat stroke model and demonstrate that this can be used for analysis of BBB integrity.

2. Results

2.1 Separation of brain vessel and parenchyma fractions

Previously published mouse brain vessels purification protocols have been used for subsequent immunofluorescence stainings and Western blotting, however, these studies usually focused on the purified vessels alone, without comparison to the remaining brain parenchyma, or using total brain homogenate for comparison. Our goal was to investigate how a modified mouse brain vessel isolation method could permit Western blot analyses of brain vessel fraction and brain parenchyma fraction from the same tissue sample. Another objective was to reduce the amount of tissue needed enough to enable investigations that require direct comparison of the two brain hemispheres from the same mouse, e.g. in stroke research.

First, we modified a previously published procedure [9] and successfully reduced tissue requirements to one mouse brain hemisphere. Specifically, volumes of liquids and centrifugation devices were scaled down, tissue was homogenized using a cannula and a small syringe instead of a dounce homogenizer, and the vessel- and myelin-depleted parenchyma fraction was collected (see Methods). At the end of the procedure, 20-80 µg of total protein could be extracted from purified vessels of one mouse brain hemisphere, which was sufficient for several Western blot experiments.

To demonstrate fractionation of wild-type mouse brains, 5 µg total protein of vessel extract or vessel-depleted parenchyma extract were subjected to Western blotting, detecting several vascular/endothelial, glial, and neuronal markers (**Fig. 1**). Vascular endothelial-specific proteins endothelial nitric oxide synthase (eNOS) and vascular-endothelial Cadherin (VE-Cadherin), as well as vascular smooth muscle cell-specific α-smooth muscle actin (α-SM-actin) were heavily enriched in the vessel fraction, demonstrating successful purification of blood vessels. By contrast, the neuronal

Preprints (www.preprints.org) | NOT PEER-REVIEWED | Posted: 16 November 2020 doi:10.20944/preprints202011.0404.v1

protein Synaptosomal-associated protein 25 (SNAP25) was mainly localized in the parenchyma fraction. Aquaporin-4 (Aqp4), which is primarily expressed in the astrocytes' vascular endfeet processes, was also distinctively enriched in the vessel fraction, indicating attachment of perivascular endfeet membranes to the purified vessels. This validates ours and other groups' previous findings showing Aqp4 immunolabelling at the surface of isolated capillaries [9, 12] and shows that endothelial cells and astrocyte endfeet processes can be purified due to their close association.

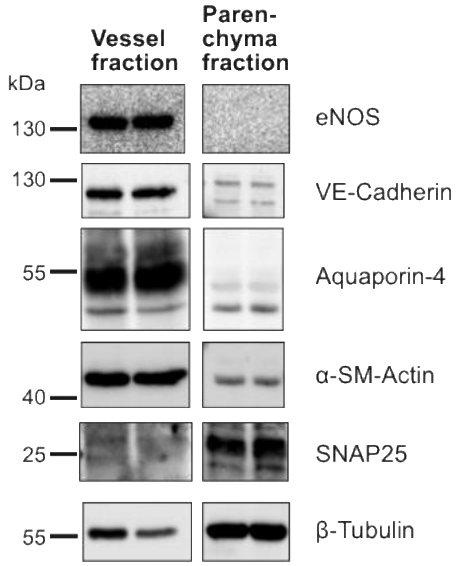

Figure 1. Separation of brain vessel and parenchyma fraction. Brain hemispheres of 2 mice were separated by centrifugation fractionation and 5 µg of total protein was subjected to SDS-PAGE and Western blotting. Vascular/endothelial markers are heavily enriched in the vessel fraction, while neuronal marker SNAP25 is detected mainly in the parenchyma fraction. α-SM-actin – α-smooth muscle actin; eNOS – endothelial nitric oxide synthase; SNAP25 – Synaptosomal-associated protein 25; VE-Cadherin – vascular endothelial Cadherin.

2.2. Use of frozen brain tissue and comparison of methods

Brain vessel isolation protocols often require the use of freshly prepared tissue [9-11], while some reports describe the use of frozen brains [13]. In order to compare tissue usability with our modified method, brains from wild-type mice were harvested and split sagitally by the interhemispheric fissure into the two hemispheres. One hemisphere was flash frozen on dry ice while the other hemisphere was processed freshly. Vessel and parenchyma fractionation was performed and several vascular endothelial-specific proteins were detected by Western blotting (**Fig. 2a).** The VE-Cadherin signal detected in the vessel fractions was lower in the frozen tissue, while signals for eNOS, α-SM-actin, and loading control β-Tubulin were comparable between freshly processed and frozen samples. This indicates that separation of vessel and parenchyma fraction can be performed equally well with both fresh and frozen tissue, however, freezing the tissue may interfere with antibody-based detection of some markers. In this experiment, we also included detection of astrocytic glial fibrillary acidic protein (GFAP), which has been detected by immunofluorescence staining in brain capillary-enriched fractions [9]. In contrast to the previously described vague signals, we found a massive enrichment of GFAP in the vessel-enriched fraction (**Fig. 2a**). When comparing freshly prepared and frozen tissue, GFAP signals were unchanged, further supporting the possibility of

Preprints (www.preprints.org) | NOT PEER-REVIEWED | Posted: 16 November 2020 doi:10.20944/preprints202011.0404.v1

using fresh and frozen tissue alike for vessel/parenchyma fractionation depending on the protein of interest.

In order to further validate and compare the efficacy of our protocol to a method that has previously been used with frozen tissue, we repeated the above experiment using a previously described vessel purification protocol [11, 13] that differs distinctly from our protocol (i.e. tissue homogenization in ammonium carbonate buffer vs. tissue homogenization in HBSS-HEPES, different centrifugation speed and length as well as absence of myelin removal step using BSA-containing buffer). Wild-type mouse brains were divided sagitally by the interhemispheric fissure, and one hemisphere was flash frozen on dry ice before performing vessel and parenchyma fractionation while the other hemisphere was processed as fresh tissue. Western blot analyses show enrichment of vascular endothelial-specific protein eNOS and vascular smooth muscle cell-specific α-SM-actin, indicating successful purification of vessels. However, signals were weaker compared to our modified method, and signals for VE-Cadherin did not confirm vascular enrichment (**Fig. 2b**). Comparison of fresh tissue with frozen tissue did not show clear differences using this method, however, GFAP signals were not enhanced in the vessel fractions as expected for a successful enrichment.

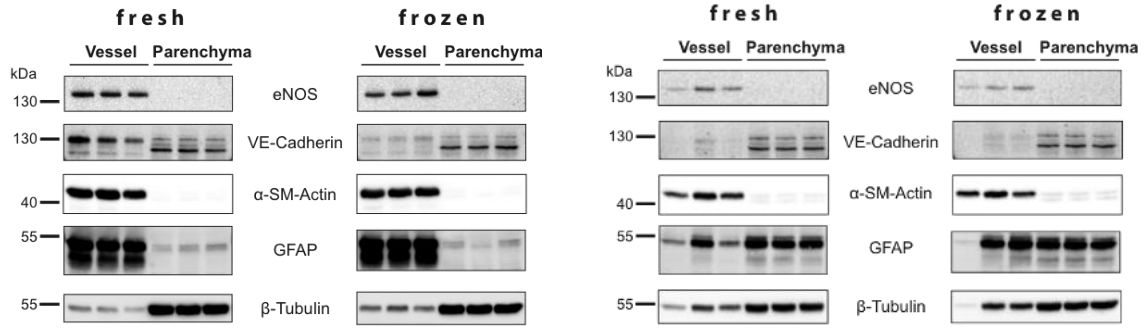

Figure 2. Comparison of fractionation methods. Harvested brains were split into hemispheres. One hemisphere was immediately subjected to vessel- and parenchyma fractionation ("fresh"), while the other hemisphere was flash frozen on dry ice and thawed before fractionation ("frozen"). 5 µg of total protein was subjected to Western blotting. Fractions generated by (**a**) the herein described method were compared to (**b**) fractions from a different protocol of cortical blood vessel isolation (Hawkes & McLaurin, 2009). α-SM-actin – α-smooth muscle actin; eNOS – endothelial nitric oxide synthase; GFAP – glial fibrillary acidic protein; VE-Cadherin – vascular endothelial Cadherin.

Taken together, our vessel and parenchyma fractionation method performed as well as previously published vessel purification methods, and required less tissue. Frozen brain tissue was generally usable for the separation by this fractionation method, with the exception of some protein targets.

2.3 Application of vessel and parenchyma fractionation in a murine stroke model

Since our modified fractionation method can be used to purify sufficient vessels from a single mouse brain hemisphere, the procedure is especially suitable for investigations in mouse models that are expected to display regional differences within the same animal. Here, we used a well-established mouse model of stroke, in which permanent occlusion of the middle cerebral artery (MCAo) causes

Preprints (www.preprints.org) | NOT PEER-REVIEWED | Posted: 16 November 2020 doi:10.20944/preprints202011.0404.v1

a lesion in the treated, ipsilateral hemisphere while the lesion-free contralateral hemisphere served as an internal control.

MCAo was performed on the left hemispheres of wild-type mice and the brains were harvested 3 days post infarct. Western blot analyses detecting serum albumin show increased signals in the ipsilateral hemisphere, both in the vessel and in the parenchyma fraction (**Fig. 3a**), indicating that the stroke-induced BBB impairment allows albumin to cross the structural barrier formed by the endothelial cells of cerebral blood vessels. Of note, the anti-albumin antibody used is specific for mouse and human albumin but does not react with bovine serum albumin, which was used during the vessel isolation procedure. Densitometric quantification of albumin signals using tubulin signals as loading controls show a 4.6-fold increase of albumin in the ipsilateral parenchyma fractions compared to the contralateral hemispheres (P = 0.003; **Fig. 3b**), thus showing that our fractionation method allowed for detection of a significant BBB dysfunction in the infarcted hemisphere.

Astrocytes that form a vital part of the BBB increase GFAP expression in response to insults, such as ischemia [14]. In our model, astrocytic GFAP expression increased 3 days post-stroke in both the vessel-enriched fractions and parenchyma-enriched fractions, which may be related to BBB destruction [15] or repair after CNS injury [16, 17] and glial scar formation to compartmentalize the site of injury [18], respectively. Western blot quantifications showed a 2.0-fold increase in GFAP signal in ipsilateral vessel fractions (P = 0.030; **Fig. 3c**), and a 1.5-fold increase in ipsilateral parenchyma fractions (P = 0.034; **Fig. 3d**), compared to contralateral fractions, respectively, demonstrating apparent astrogliosis in both vessel and parenchyma compartment. This application confirms that vessel- and parenchyma fractionation can be applied in experiments using single mouse brain hemispheres, allowing for quantitative comparisons between hemispheres of both brain vessel and brain parenchyma fractions.

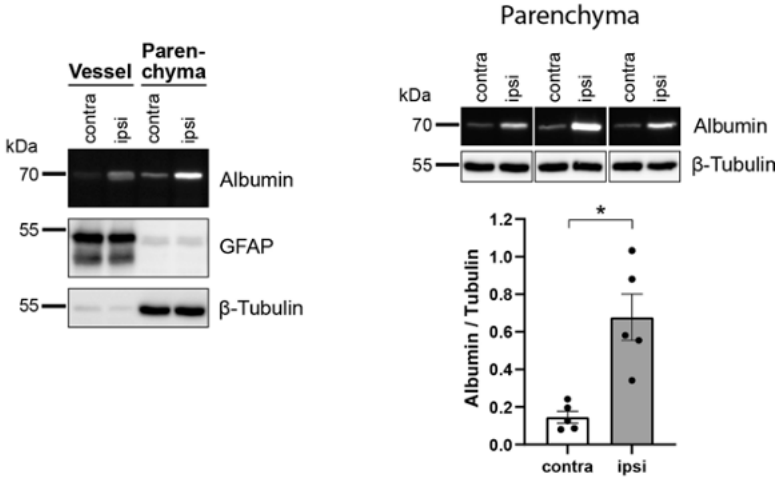

(a) **(b)**

Preprints (www.preprints.org) | NOT PEER-REVIEWED | Posted: 16 November 2020 doi:10.20944/preprints202011.0404.v1

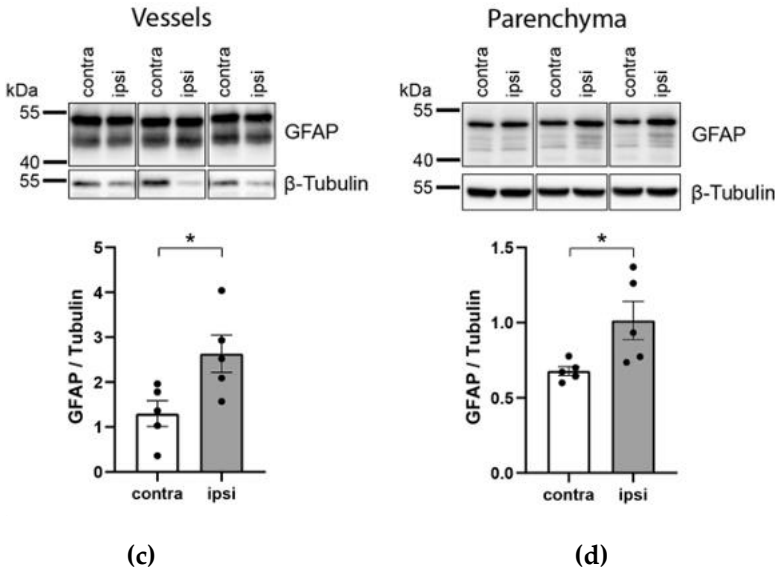

Figure 3. Application of vessel/parenchyma fractionation in a murine stroke model. Wild-type mice were subjected to permanent occlusion of the left middle cerebral artery. After 3 days brains were harvested and separated into the lesion-containing ipsilateral and the contralateral hemispheres. Vessel- and parenchyma fractionation was performed and 5 µg of total protein was subjected to Western blotting. (**a**) A mouse- and human-specific anti-albumin antibody shows increase of albumin in the ipsilateral fractions. GFAP is mainly contained in the vessel fractions. (**b**) Parenchyma fractions of stroke mice show significant increase of albumin in the ipsilateral hemisphere, indicating hemisphere-specific BBB impairment. n = 5, mean ± SEM, t-test $P < 0.05$. GFAP expression was increased in the ipsilateral hemispheres, both in vessel fractions (**c**) and in parenchyma fractions (**d**). n = 5, mean ± SEM, t-test $P < 0.05$. contra – contralateral (lesion-free) hemisphere, ipsi – ipsilateral (ischemic) hemisphere, GFAP – glial fibrillary acidic protein.

2.4 Application of vessel- and parenchyma fractionation in a rat stroke model

To test whether our vessel- and parenchyma fractionation protocol is also applicable to rat brains, we used a recently-described thromboembolic stroke model [19]. Stroke was induced by local injection of α-thrombin into the lumen of the middle cerebral artery of wild-type rats. Brains were harvested 24 h after stroke induction and separated into the lesion-containing ipsilateral and the contralateral hemispheres. Vessel and parenchyma fractionation was performed using 3-fold increased volumes to account for the larger rat brains, and the resulting samples were subjected to Western blotting. Vessel fractions displayed strong enrichments of vascular endothelial protein VE-Cadherin and vascular smooth muscle cell-specific α-SM-actin, indicating successful vessel purification (**Fig. 4a**). Of note, anti-eNOS antibody (ab76198, Abcam, UK) did not react with rat protein (data not shown). Similar to our experiments in mice, a strong signal of astrocytic GFAP was detected in the vessel-enriched fraction, and albumin signals were more pronounced in the parenchyma fraction. To evaluate stroke-induced BBB leakiness, parenchyma fractions of ipsi- and contralateral hemispheres were subjected to Western blotting. Densitometric analyses of albumin signals using tubulin signals as loading controls show a 4.6-fold increase in the ipsilateral compared to the contralateral fractions (P = 0.021; **Fig. 4b**).

Preprints (www.preprints.org) | NOT PEER-REVIEWED | Posted: 16 November 2020 doi:10.20944/preprints202011.0404.v1

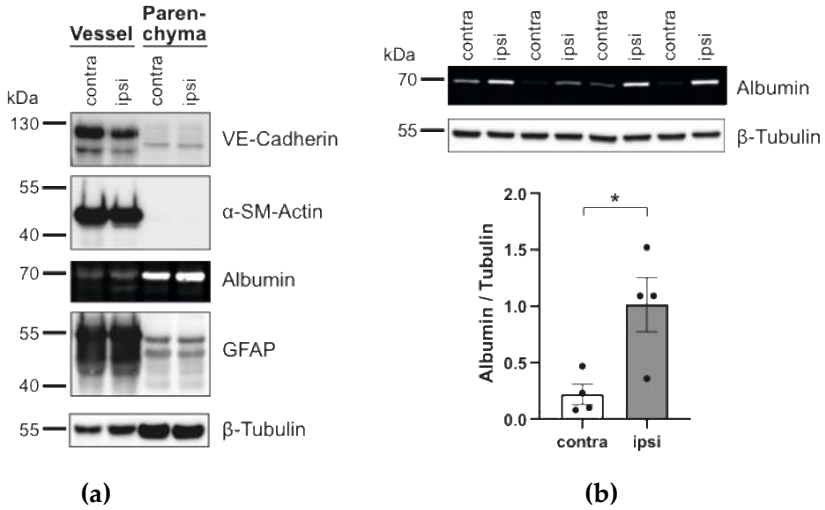

Figure 4. Demonstration of vessel- and parenchyma fractionation in a thromboembolic stroke model in rats. Rat brains were harvested 24 h after thrombin-induced stroke and separated into the lesion-containing ipsilateral and the contralateral hemispheres. Vessel- and parenchyma fractionation was performed and 10 µg of total protein was subjected to Western blotting. (**a**) Enrichment of vascular/endothelial markers and GFAP in the vessel fractions. (**b**) Parenchyma fractions of stroke rats showed significant increase of albumin in the ipsilateral hemisphere, indicating hemisphere-specific BBB impairment. n = 4, mean ± SEM, t-test $P < 0.05$. contra – contralateral (lesion-free) hemisphere, ipsi – ipsilateral (ischemic) hemisphere, VE-Cadherin – vascular endothelial Cadherin; α-SM-actin – α-smooth muscle actin; GFAP – glial fibrillary acidic protein.

Despite the considerable variation, especially between ipsilateral signals and the different method of stroke induction, this increase very accurately matches the ipsilateral increase of albumin measured in the mouse stroke experiments. This highlights the validity of centrifugation-based separation of tissue into vessel- and parenchyma-enriched fractions both across species and in healthy and disease conditions and demonstrates a new application for investigations of BBB dysfunction.

3. Discussion

In this study, we evaluated a modified mouse brain vessel isolation method that permits quantitative protein analyses of brain vessel and brain parenchyma fractions and thus, enables investigations requiring analysis of small tissue volumes, e.g. the direct comparison of the two brain hemispheres from the same animal. The method is based on a mechanical vessel isolation procedure [9], and does not require density gradient centrifugation or enzymatic digestion, rendering it technically straight-forward and more reproducible. Previous studies using similar vessel isolation protocols have mainly focused on the purified vessel fraction alone [9, 20, 21] or compared the purified vessels to total brain homogenate [10, 22], necessitating two tissue samples. Our approach has the advantage of enabling comparison of the vessel fraction to the parenchyma fraction of the same mouse brain sample, which has previously only been performed with larger tissue quantities, i.e. human material [23]. We demonstrated the applicability of our modified method in a murine stroke model where it allows the reliable quantification of serum-albumin accumulation in brain parenchyma of the ipsilateral hemisphere as well as the quantitative comparison of astrogliosis both in vessel and parenchyma fraction. We furthermore validated the method in a rat model of stroke. Thus, our results show that this method serves as an un-biased way of detecting BBB dysfunction and alterations in the neurovascular niche.

 doi:10.20944/preprints202011.0404.v1

The use of frozen tissue samples for brain vessel isolation has been described [13, 23, 24], but the literature remains elusive about the effects of freezing or simply claim to require fresh tissue. We directly compared vessel fractionation using fresh and dry-ice frozen brain tissue, demonstrating general usability of frozen brain tissue for fractionation, although some protein targets, such as VE-Cadherin, may be affected by the freezing process.

BBB integrity is an important target for assessment in studies of neurodegeneration and has an important role in the evaluation of treatment [25-29]. BBB breakdown is widely assessed using microscopy analyses following FITC-albumin or Evans Blue (EB) extravasation into the brain parenchyma. Despite its limitations, EB with its albumin-binding capacity is still the most commonly used tracer for such studies [30]. For both EB and FITC-labeled tracers, animals need to be perfused after injection and circulation of the dyes, which prevents the use of blood or plasma for additional readouts (e.g., flow cytometry, Elisa etc.). Moreover, histology quantification is associated to artefacts due to tissue preparation that requires fixation or accompanying autofluorescence. Commonly employed histological methods are subject to observer bias and are not amenable to rigorous quantitative analysis. Our study shows that BBB integrity can be assayed by analysis of serum albumin in the parenchymal-enriched fractions after centrifugation separation of brain tissue, adding another option for quantitatively studying BBB dysfunction. Additional, compartmentalization of blood vessels and brain parenchyma using the herein described protocol allows for further quantitative assessment of molecular contributors to BBB impairment of interest (e.g., tight junction and adherens junction proteins) [31, 32].

During stroke, the ionic imbalance caused by disruption of oxygen supply to the brain rapidly activates proteolytic enzymes, which negatively affect the BBB [8]. In experimental stroke research, fluorescently labelled dextran or albumin as well as EB are the gold-standard methods to assess BBB impairment with the above-mentioned shortcomings. With our centrifugation-based fractionation method we provide a quantitative and versatile method that allows for detection of BBB dysfunction in the infarcted hemisphere using Western blot approaches that permits comparing to the lesion-free contralateral hemisphere from the same animal which serves as an internal control. Our data provide compelling validation of our method by showing significantly increased serum-albumin protein expression in both the ipsilateral parenchyma fractions, suggestive of apparent BBB leakiness 3 days post-stroke in a murine model as well as 1-day post-stroke in a rat model. In stroke lesion formation, the loss of BBB integrity was shown to not only associate to the deregulation of tight junction proteins but also coincides with perivascular astrogliosis [15]. The significantly augmented GFAP protein expression observed in the ipsilateral vessel fraction compared to the lesion-free contralateral control evidences apparent astrogliosis [14] that may link to impairments of BBB integrity mediated through the release of vascular permeability factors such as, vascular endothelial growth factor [33], matrix metalloproteinases [34], endothelin [35], nitric oxide [36] or glutamate [37]. Alternatively, augmented astrogliosis associated to the cerebral vasculature may also point towards regenerative processes during the chronic phase post-stroke as astrocytes release vascular protective substances, including glial-derived neurotrophic factor [38, 39], insulin-like growth factor-1 [40] or Apolipoprotein E [41, 42]. The concurrent significantly higher serum-albumin expression detected in the ipsilateral parenchyma fraction, however, points to a leaky BBB and thus, suggests astrogliosis linked to BBB destruction rather than protection 3 days post-stroke.

Preprints (www.preprints.org) | NOT PEER-REVIEWED | Posted: 16 November 2020 doi:10.20944/preprints202011.0404.v1

Studies demonstrated that astrocyte responses to injury encompass a broad continuum of cellular changes [43], ranging from mild insults that may result in the upregulation of GFAP expression in a subset of astrocytes that do not express GFAP at appreciable levels under physiologic conditions to moderate or severe GFAP upregulation and hypertrophy. Histological assessment of GFAP$^+$ astrocytes is widely accepted, however, counting reactive astrocytes can be challenging due to extensive process thickening, elongation, ramification, and overlap, which potentially adds variability to the results thus, permitting reliable quantitative assessments. Our method provides an opportunity to quantify the degree of astroglial activation (e.g., during disease progression and regeneration after cerebral infarction) and additionally provides a certain degree of spatial information (i.e. vessel vs. parenchyma-associated astrogliosis) through quantitative western blot-based evaluation of for instance, GFAP expression. Western blotting of vessel- and parenchyma enriched fractions could thus be an unbiased alternative to traditional cell counting.

Taken together, our study validates a modified protocol for centrifugation-based vessel and parenchyma fraction separation from a single mouse brain hemisphere for reliable quantitative assessment of BBB integrity and the neurovascular niche.

4. Materials and Methods

4.1 Chemicals and reagents

All chemical reagents and solutions were purchased from Fisher Scientific (Göteborg, Sweden), Saveen & Werner (Limhamn, Sweden) or Sigma-Aldrich (Stockholm, Sweden) unless otherwise stated. Commercially available primary antibodies against VE-Cadherin, eNOS and SNAP-25 (Abcam, UK), GFAP (Dako, Agilent, Sweden), beta-tubulin and alpha-SMA (Sigma, Sweden), and human/mouse serum-albumin (Biotechne, UK) were used for immunodetection. Donkey anti-mouse and donkey anti-rabbit HRP-coupled secondary antibodies or Alexa Fluor 680 donkey anti-goat (Nordic Biosite, Sweden) secondary antibodies were used for visualization.

4.2 Animals

This investigation conforms to the Guide for Care and Use of Laboratory Animals published by the European Union (Directive 2010/63/EU) and with the ARRIVE guidelines. All animal care and experimental protocols were approved by the institutional animal ethics committee at Lund University (Dnr.: 5.8.18-12657/2017 and 5.8.18-10593/2020) and were conducted in accordance with European animal protection laws. Wild type C57Bl/6N were obtained from Taconic (Ejby, Denmark) and housed in a conventional animal facility under standard conditions with a 12:12 h light-dark cycle and access to food (standard rodent diet) and water *ad libitum*. Mice were housed in groups of four to five in conventional transparent polycarbonate cages. Rats were housed in groups of two in conventional transparent polycarbonate cages.

4.3 Permanent middle cerebral artery occlusion (MCAo) in mice

Three-months old male mice were anesthetized with isofluorane (IsoFlo® vet 100%; Abbott, Sweden, 2% at 1.5L/min in room air) using a vaporizer (Tec-3, Cyprane Ltd., Keighley, UK). During the procedure, the body temperature was maintained at 36.5 ± 0.5 °C. Between the orbit and the external auditory meatus 1 cm skin incision was made and the temporal muscle was separated from the skull

Preprints (www.preprints.org) | NOT PEER-REVIEWED | Posted: 16 November 2020 doi:10.20944/preprints202011.0404.v1

by electrocoagulation forceps (ICC50, Erbe, Germany). The MCA bifurcation was identified and 1-2 mm hole was drilled above it in the rostral part of the temporal area. The proximal part of the MCA was occluded by short electrocoagulation followed by transection of the vessel to ensure the permanent occlusion. The temporal muscle was placed to its original position and wound was sutured. Following surgery, animals received intraperitoneal injections of Buprenorphine (0,1 mg/kg) for pain relief and subcutaneous injection of saline to prevent dehydration.

4.4. Thromboembolic stroke in rats

Thromboembolic stroke was induced by local injection of α-thrombin directly into the lumen of the right middle cerebral artery (MCA) in male Wistar rats (299-385 g; Janvier, France) as recently described [19]. Rats were anesthetized using 3% isoflurane and maintained with 1.5-2% isoflurane in N_2O:O_2 (70:30). An electric temperature probe was inserted into the rectum of the rat to record the temperature, and found to be maintained at 37ºC. The rat was placed in a stereotactic device and the temporal muscle was retracted. A craniectomy was performed, the dura was excised, and the MCA was exposed. The laser Doppler flow probe (AD Instruments, UK) was placed over the MCA territory for monitoring the CBF during the duration of the surgery. A micropipette filled with 12 UI human α-thrombin (4 UI/µl, Nordic Diagnostica AB, Sweden) was introduced into the lumen of the MCA bifurcation and injected carefully to induce the formation of a clot *in situ*. The pipette was removed 20 minutes after the injection at which time the clot had stabilized. To minimize suffering, the rats received Marcaine (1.25 mg/kg, AstraZeneca) at the site of incisions as analgesics and eye gel (Viscotears) to prevent the cornea from drying out during surgery procedure. A subcutaneous injection of 10 ml of isotonic saline for rehydration was given at the end of the surgery.

4.5 Brain vessel-parenchyma fractionation

Brain vessels were separated from parenchyma by a procedure modified from Boulay *et al.* [9]. The original protocol was scaled down for use with one mouse brain hemisphere [or one rat brain hemisphere]. Animals were transcardially perfused with PBS and brains were collected on ice. All buffers were precooled on ice. One brain hemisphere was minced to small pieces with a scalpel in 1 ml B1 (HBSS with 10 mM HEPES) [rat: 3 ml]. The sample was homogenized using a long 21G cannula (0.8 x 120 mm) mounted on a 2 ml syringe [rat: 5 ml syringe] by aspirating and pushing out 20 times. The homogenate was transferred to a 2 ml tube [rat: 15 ml tube] and centrifuged in a fixed-angle rotor at 2,000 g and 4 °C for 10 min. The supernatant, representing the parenchyma fraction, was taken off and mixed with an equal volume of 2x RIPA buffer including protease and phosphatase inhibitor cocktails before freezing on dry ice and storing at -80 °C. The pellet containing the vessels was resuspended in 2 ml B2 (B1 with 18 % (w/v) dextran, M_r ≈70,000) [rat: 6 ml] by vigorous shaking, and centrifuged at 4,400 g and 4 °C for 15 min. The supernatant including the myelin layer was carefully removed and the pellet was resuspended in 1 ml B3 (B1 with 1 % (w/v) BSA). Brain vessels were collected on a 20 µm mini cell strainer (pluriSelect, Leipzig, Germany) by centrifugation at 200 g for 1 min in a swinging-bucket rotor. Vessels were washed twice by resuspending in 1 ml B3 on the strainer and subsequent centrifugation. The purified vessels were taken up in 1 ml B3 by rinsing the strainer, transferred to a 1.5 ml tube, and sedimented at 2,000 g and 4 °C for 5 min. To remove BSA the supernatant was discarded and the pellet was carefully resuspended in 1 ml B1, followed by centrifugation at 2,000 g and 4 °C for 5 min. Supernatant was removed completely and the vessels were frozen on dry ice and stored at -80°C.

 doi:10.20944/preprints202011.0404.v1

4.6 Western Blotting

To extract proteins purified vessels were thawed by mixing with 100 µl RIPA buffer containing 10 mM Tris (pH 8.0), 1 mM EDTA, 1 % Triton X-100, 0.1 % sodium deoxycholate, 0.1 % SDS, 140 mM NaCl and protease and phosphatase inhibitor cocktails (Merck, Darmstadt, Germany), and homogenized in a glass micro homogenizer (Radnoti, Dublin, Ireland) with at least 20 strokes. Parenchyma samples, which had been frozen after mixing with 2x RIPA buffer, were thawed on ice. Vessel and parenchyma samples were mixed vigorously, incubated on ice for 30 min, mixed vigorously again, and insoluble material was removed by centrifugation at 20,000 g and 4 °C for 10 min. Protein concentration was determined by Pierce BCA protein assay (Fisher Scientific, Sweden). Western blotting was carried out according to standard protocols. Briefly, samples were mixed with 4x sample buffer (0.2 M Tris pH 6.8, 8 % SDS, 40 % (v/v) glycerol, 20 % (v/v) β-mercaptoethanol, 0.02 % (w/v) bromophenol blue) and heated for 10 min at 95 ºC. Proteins were separated on 10 % or 12 % SDS-PAGE mini gels and transferred onto PVDF membranes (Biorad, Sweden). Membranes were blocked for 30 min in 1 % bovine serum albumin (in phosphate-buffered saline containing 1 % Tween-20 (PBST); 137 mM NaCl, 2.7 mM KCl, 10 mM Na_2HPO_4, 1.8 mM KH_2PO_4; pH 7.4) and sequentially incubated with the primary and secondary antibodies. An antibody-specific dilution for the primary antibodies, and 1:10,000 for the HRP-labeled secondary antibody were utilized. All antibodies were diluted in 1 % bovine serum albumin or 5 % milk in PBST. A standard chemiluminescence procedure (ECL Plus) was used to visualize protein binding. The developed membranes were evaluated densitometrically using Image Lab 6.0.1 (Biorad, Sweden).

4.7 Statistics

All data are expressed as mean ± SEM, where n is the number of animals. For comparison of two groups a two-tailed unpaired t-test was utilized. Differences were considered significant at error probabilities of $P \leq 0.05$.

Author Contributions: Conceptualization, AM and IL; methodology, FM; validation, FM and HM; formal analysis, FM and AM; data curation, FM, HM, KA; writing—original draft preparation, FM, AM, IL; writing—review and editing, FM, HM, AM, IL.; visualization, FM; supervision, AM; project administration, AM; funding acquisition, AM, IL and SA. All authors have read and agreed to the published version of the manuscript.

Funding: This work was supported by the following funding sources: The Knut and Alice Wallenberg foundation [F 2015/2112, AM, IL]; Swedish Research Council [VR; 2017-01243, AM; 2018-02340, IL]; Crafoord Foundation [IL, SA], German Research Foundation [DFG; ME 4667/2-1; AM], Strokeriksförbundet [AM], Sparbanken Skåne [AM, SA], Brain Foundation [SA], Hedlund Stiftelse [M-2019-1101; AM], Åke Wibergs Stiftelse [M19-0380; AM] and Demensfonden [AM].

Conflicts of Interest: The authors declare no conflict of interest.

Abbreviations

a-SM actin	Alpha smooth muscle actin
Aqp4	Aquaporin-4
BBB	Blood Brain Barrier
contra	Contralateral
eNOS	Endothelial nitric oxide synthase
GFAP	Glial fibrillary acidic protein
Ipsi	Ipsilateral
MCAo	Middle cerebral artery occlusion
SNAP25	Synaptosomal-associated protein 25
VE-Cadherin	Vascular endothelial Cadherin

References

1. Daneman, R. and A. Prat, *The blood-brain barrier.* Cold Spring Harb Perspect Biol, 2015. **7**(1): p. a020412.
2. Pardridge, W.M., *Blood-brain barrier delivery.* Drug Discov Today, 2007. **12**(1-2): p. 54-61.
3. Sweeney, M.D., et al., *The role of brain vasculature in neurodegenerative disorders.* Nat Neurosci, 2018. **21**(10): p. 1318-1331.
4. Di Giovanna, A.P., et al., *Whole-Brain Vasculature Reconstruction at the Single Capillary Level.* Sci Rep, 2018. **8**(1): p. 12573.
5. Abbott, N.J., *Blood-brain barrier structure and function and the challenges for CNS drug delivery.* J Inherit Metab Dis, 2013. **36**(3): p. 437-49.
6. Yu, X., C. Ji, and A. Shao, *Neurovascular Unit Dysfunction and Neurodegenerative Disorders.* Front Neurosci, 2020. **14**: p. 334.
7. Ahmad, A., et al., *The Role of Neurovascular System in Neurodegenerative Diseases.* Mol Neurobiol, 2020. **57**(11): p. 4373-4393.
8. Krueger, M., et al., *Endothelial edema precedes blood-brain barrier breakdown in early time points after experimental focal cerebral ischemia.* Acta Neuropathol Commun, 2019. **7**(1): p. 17.
9. Boulay, A.C., et al., *Purification of Mouse Brain Vessels.* J Vis Exp, 2015(105): p. e53208.
10. Lee, Y.K., et al., *The isolation and molecular characterization of cerebral microvessels.* Nat Protoc, 2019. **14**(11): p. 3059-3081.
11. Hawkes, C.A. and J. McLaurin, *Selective targeting of perivascular macrophages for clearance of beta-amyloid in cerebral amyloid angiopathy.* Proc Natl Acad Sci U S A, 2009. **106**(4): p. 1261-6.
12. Munk, A.S., et al., *PDGF-B Is Required for Development of the Glymphatic System.* Cell Rep, 2019. **26**(11): p. 2955-2969 e3.
13. Joo, I.L., et al., *Early neurovascular dysfunction in a transgenic rat model of Alzheimer's disease.* Sci Rep, 2017. **7**: p. 46427.
14. Becerra-Calixto, A. and G.P. Cardona-Gomez, *The Role of Astrocytes in Neuroprotection after Brain Stroke: Potential in Cell Therapy.* Front Mol Neurosci, 2017. **10**: p. 88.
15. Alvarez, J.I., et al., *Focal disturbances in the blood-brain barrier are associated with formation of neuroinflammatory lesions.* Neurobiol Dis, 2015. **74**: p. 14-24.
16. Kubotera, H., et al., *Astrocytic endfeet re-cover blood vessels after removal by laser ablation.* Sci Rep, 2019. **9**(1): p. 1263.
17. Hayakawa, K., et al., *Reactive astrocytes promote adhesive interactions between brain endothelium and endothelial progenitor cells via HMGB1 and beta-2 integrin signaling.* Stem Cell Res, 2014. **12**(2): p. 531-8.
18. Anderson, M.A., et al., *Astrocyte scar formation aids central nervous system axon regeneration.* Nature, 2016. **532**(7598): p. 195-200.
19. Arkelius, K., et al., *Validation of a stroke model in rat compatible with rt-PA-induced thrombolysis: new hope for successful translation to the clinic.* Sci Rep, 2020. **10**(1): p. 12191.

20. Begum, G., et al., *Selective knockout of astrocytic Na(+) /H(+) exchanger isoform 1 reduces astrogliosis, BBB damage, infarction, and improves neurological function after ischemic stroke.* Glia, 2018. **66**(1): p. 126-144.
21. Yanagida, K., et al., *Size-selective opening of the blood-brain barrier by targeting endothelial sphingosine 1-phosphate receptor 1.* Proc Natl Acad Sci U S A, 2017. **114**(17): p. 4531-4536.
22. Gama Sosa, M.A., et al., *Low-level blast exposure disrupts gliovascular and neurovascular connections and induces a chronic vascular pathology in rat brain.* Acta Neuropathol Commun, 2019. **7**(1): p. 6.
23. Bourassa, P., et al., *Beta-amyloid pathology in human brain microvessel extracts from the parietal cortex: relation with cerebral amyloid angiopathy and Alzheimer's disease.* Acta Neuropathol, 2019. **137**(5): p. 801-823.
24. Pardridge, W.M., et al., *Isolation of intact capillaries and capillary plasma membranes from frozen human brain.* J Neurosci Res, 1987. **18**(2): p. 352-7.
25. Corem, N., et al., *Leptin receptor deficiency induces early, transient and hyperglycaemia-independent blood-brain barrier dysfunction.* Sci Rep, 2019. **9**(1): p. 2884.
26. Di Pardo, A., et al., *Impairment of blood-brain barrier is an early event in R6/2 mouse model of Huntington Disease.* Sci Rep, 2017. **7**: p. 41316.
27. Gustafsson, S., et al., *Blood-brain barrier integrity in a mouse model of Alzheimer's disease with or without acute 3D6 immunotherapy.* Neuropharmacology, 2018. **143**: p. 1-9.
28. Salas-Perdomo, A., et al., *Role of the S1P pathway and inhibition by fingolimod in preventing hemorrhagic transformation after stroke.* Sci Rep, 2019. **9**(1): p. 8309.
29. Meissner, A., et al., *Structural and functional brain alterations in a murine model of Angiotensin II-induced hypertension.* J Neurochem, 2017. **140**(3): p. 509-521.
30. Saunders, N.R., et al., *Markers for blood-brain barrier integrity: how appropriate is Evans blue in the twenty-first century and what are the alternatives?* Front Neurosci, 2015. **9**: p. 385.
31. Wimmer, I., et al., *PECAM-1 Stabilizes Blood-Brain Barrier Integrity and Favors Paracellular T-Cell Diapedesis Across the Blood-Brain Barrier During Neuroinflammation.* Front Immunol, 2019. **10**: p. 711.
32. Winger, R.C., et al., *Rapid remodeling of tight junctions during paracellular diapedesis in a human model of the blood-brain barrier.* J Immunol, 2014. **193**(5): p. 2427-37.
33. Argaw, A.T., et al., *Astrocyte-derived VEGF-A drives blood-brain barrier disruption in CNS inflammatory disease.* J Clin Invest, 2012. **122**(7): p. 2454-68.
34. Min, H., et al., *TLR2-induced astrocyte MMP9 activation compromises the blood brain barrier and exacerbates intracerebral hemorrhage in animal models.* Mol Brain, 2015. **8**: p. 23.
35. Yeung, P.K., et al., *Targeted over-expression of endothelin-1 in astrocytes leads to more severe brain damage and vasospasm after subarachnoid hemorrhage.* BMC Neurosci, 2013. **14**: p. 131.
36. Liu, B. and A.H. Neufeld, *Expression of nitric oxide synthase-2 (NOS-2) in reactive astrocytes of the human glaucomatous optic nerve head.* Glia, 2000. **30**(2): p. 178-86.
37. Lu, L., et al., *Astrocytes drive cortical vasodilatory signaling by activating endothelial NMDA receptors.* J Cereb Blood Flow Metab, 2019. **39**(3): p. 481-496.

 doi:10.20944/preprints202011.0404.v1

38. Chen, M., et al., *Glial Cell Line-Derived Neurotrophic Factor (GDNF) Promotes Angiogenesis through the Demethylation of the Fibromodulin (FMOD) Promoter in Glioblastoma.* Med Sci Monit, 2018. **24**: p. 6137-6143.
39. Xiao, W., et al., *GDNF is involved in the barrier-inducing effect of enteric glial cells on intestinal epithelial cells under acute ischemia reperfusion stimulation.* Mol Neurobiol, 2014. **50**(2): p. 274-89.
40. Okoreeh, A.K., S. Bake, and F. Sohrabji, *Astrocyte-specific insulin-like growth factor-1 gene transfer in aging female rats improves stroke outcomes.* Glia, 2017. **65**(7): p. 1043-1058.
41. Cao, F., et al., *Apolipoprotein E-Mimetic COG1410 Reduces Acute Vasogenic Edema following Traumatic Brain Injury.* J Neurotrauma, 2016. **33**(2): p. 175-82.
42. Teng, Z., et al., *ApoE Influences the Blood-Brain Barrier Through the NF-kappaB/MMP-9 Pathway After Traumatic Brain Injury.* Sci Rep, 2017. **7**(1): p. 6649.
43. Anderson, M.A., Y. Ao, and M.V. Sofroniew, *Heterogeneity of reactive astrocytes.* Neurosci Lett, 2014. **565**: p. 23-9.